Natural formation of copper sulfide nanoparticles via microbially mediated organic sulfur mineralization in soil: processes and mechanisms

Xu, H.; Zhang, P.; He, E.; Peijnenburg, W.J.G.M.; Cao, X.; Zhao, L.; ... ; Qiu, H.

Geoderma 430 (2023) 116300

Contents lists available at ScienceDirect

Geoderma

journal homepage: www.elsevier.com/locate/geoderma

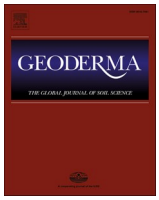

Natural formation of copper sulfide nanoparticles via microbially mediated organic sulfur mineralization in soil: Processes and mechanisms

Hang Xu [a], Peihua Zhang [a], Erkai He [b], Willie J.G.M. Peijnenburg [c,d], Xinde Cao [a], Ling Zhao [a], Xiaoyun Xu [a], Hao Qiu [a,*]

[a] School of Environmental Science and Engineering, Shanghai Jiao Tong University, Shanghai 200240, China
[b] School of Geographic Sciences, East China Normal University, 200241 Shanghai, China
[c] National Institute of Public Health and the Environment, Center for the Safety of Substances and Products, 3720BA Bilthoven, the Netherlands
[d] Institute of Environmental Sciences, Leiden University, 2300RA Leiden, the Netherlands

ARTICLE INFO

Handling Editor: Naoise Nunan

Keywords:
Copper sulfide
Sulfur
Metal transformation
Metagenomics
Paddy soil

ABSTRACT

Sulfur cycling is known to control the speciation and bioavailability of copper in the environment via inorganic sulfur oxidation and reduction. However, it remains unclear how the mineralization of organic sulfur and associated microbial processes affect Cu transformations. This study discovered a neglected mechanism that mediates Cu mobility and speciation via cysteine mineralization in a paddy soil. We provide evidence for a pathway of sulfide production from cysteine via indigenous soil microorganisms. The produced sulfide promotes the formation of copper sulfide nanoparticles, constituting an alternative copper sulfide formation mechanism that bypasses sulfate reduction. A bacterium isolated from the soil, named *Bacillus* sp. TR1, played a role in forming cell-associated copper sulfide nanoparticles. A metagenomics approach was applied to detect genes related to cysteine mineralization (*dcyD*, *CTH*, *CBS*, and *sseA*) and the associated microbes in the soil. The *sseA* gene was most abundant, and the microorganisms involved in cysteine mineralization were taxonomically diverse, including members of phyla *Proteobacteria*, *Firmicutes*, and *Thaumarchaeota*. *Geobacter*, *Sulfuriferula*, *Nitrososphaera*, *Noviherbaspirillum*, and *Clostridium* were the dominant genera with potential to metabolize cysteine to form copper sulfide nanoparticles. Our study not only provides initial molecular-level insights into the abundance, diversity, and metabolism of cysteine-mineralizing microorganisms but also highlights their important ecological functions in metal and sulfur biogeochemical cycles.

1. Introduction

Copper (Cu) is an important trace element required as a redox cofactor by many proteins and enzymes that carry out fundamental biological functions in living organisms (Rubino and Franz, 2012). As a result, Cu is involved in various biogeochemical processes such as denitrification and methane oxidation (Averill, 1996; Semrau et al., 2010). However, excessive Cu derived from anthropogenic sources has detrimental effects on soil biota and ecosystem functioning (Baath, 1989). The mobility and bioavailability of Cu in soils are controlled by both biotic and abiotic factors. Among these factors, microbe-assisted sulfur biogeochemical cycling in soils can significantly influence the speciation and solubility of Cu according to sulfur oxidation/reduction reactions (Jorgensen et al., 2019).

Sulfur oxidizing bacteria (SOB) can use reductive sulfur compounds, such as sulfide and zero-valent sulfur, as energy sources for growth. This induces the release of metal ions via mineral dissolution in the sulfuric acid that is produced (Hou et al., 2020; Zhang et al., 2020). The production of sulfate through sulfur oxidation can further increase sulfur bioavailability and support the metabolism of sulfate-reducing bacteria (SRB), which utilize sulfate as an electron acceptor and generate hydrogen sulfide while oxidizing organic matter (Bell et al., 2020). The biologically produced hydrogen sulfide facilitates the precipitation of metals as low-mobility sulfides. This can be used as an important strategy to constrain metal bioavailability.

Organic sulfur is the main sulfur (S) fraction in soils. It comprises >90 % of the total S in most surface soils and as much as 99 % in subsurface soils (Kertesz and Mirleau, 2004; Wilhelm Scherer, 2009). Synchrotron-based X-ray absorption near-edge structure (XANES) spectroscopy shows that there are two major groups of organic sulfur in

* Corresponding author.
E-mail address: haoqiu@sjtu.edu.cn (H. Qiu).

https://doi.org/10.1016/j.geoderma.2022.116300
Received 18 May 2022; Received in revised form 18 November 2022; Accepted 1 December 2022
Available online 8 December 2022

soils: oxidized organic sulfur (such as sulfoxide, sulfone, sulfonate, and ester sulfate) and reduced organic sulfur (such as mono- and disulfide) (Prietzel et al., 2011; Prietzel et al., 2007). The organic sulfur can be transformed into inorganic sulfur via microbial mineralization processes (Wilhelm Scherer, 2009). A non-steady-state early diagenetic model has been developed, which shows that the hydrolysis of organic ester-sulfates provides an additional source of sulfate in lake sediments (Couture et al., 2016). Likewise, the mineralization of reduced organic sulfur compounds produces sulfides to support sedimentary pyrite precipitation, which provides a more important input of inorganic sulfur (Fakhraee and Katsev, 2019). Unfortunately, such organic sulfur mineralization processes in soil have received less attention than inorganic sulfur cycle processes such as sulfur oxidation and reduction. Their biogeochemical reactions with heavy metals in the environment have received even less attention.

A representative metabolite of reduced organic sulfur is cysteine (Cys), which is ubiquitous in terrestrial and aquatic environments (Fakhraee and Katsev, 2019; Moran and Durham, 2019). Emissions of hydrogen sulfide (H_2S) have been detected in cysteine- and cystine-amended paddy soils due to substrate mineralization processes other than sulfate reduction (Morra and Dick, 1989; Swaby and Fedel, 1973). The associated enzymes (e.g., cysteine desulfhydrase, cystathionine γ-lyase, cystathionine β-synthase, and 3-mercaptopyruvate sulfurtransferase together with cysteine aminotransferase) are responsible for the generation of H_2S from cysteine (Morra and Dick, 1991; Shatalin et al., 2011). Previous studies show that Cys can act as a reducing agent and as a ligand to affect metal speciation (Walsh et al., 2015). Only a few studies have considered the impact of the degradation of cysteine to sulfide on metal transformation. For example, bacteria such as *Escherichia coli*, *Bacillus subtilis*, and *Geobacter sulfurreducens* in pure culture can participate in the formation of mercury sulfide due to the degradation of cysteine (Thomas et al., 2018). This evidence suggests that organic sulfur metabolites, such as Cys, play an important role in the biogeochemical cycles of heavy metals in soils. However, our knowledge of metal transformation processes and mechanisms related to cysteine mineralization in soil environments remains incomplete. Moreover, the underlying microbial metabolic pathways along with the associated microbes need to be elucidated.

The present study, therefore, aims to investigate the processes and mechanisms of cysteine mineralization involved in the sulfur cycle and copper transformation in a paddy soil. Microbes participating in cysteine mineralization were identified to analyze their diversity, abundance and metabolic potentials. In particular, we explored the effect of cysteine mineralization on (i) sulfide production and consumption, (ii) dissolved trace metal dynamics and (iii) copper sulfide nanoparticle formation and morphology. Combined geomicrobiological and metagenomic approaches were used to measure the key functional gene abundance involved in sulfur transformation, and to determine the microorganisms involved in copper sulfide formation via the cysteine mineralization pathway.

2. Materials and methods

2.1. Soil incubation

Soil samples were collected from the top 20 cm of soil at a rice paddy site in Changshu, Jiangsu, China. After collection, the soil samples were air-dried and passed through a 2 mm sieve. The physicochemical properties of the paddy soil are shown in Table S1. Soil incubation experiments were set up by adding 2 g of soil to a serum vial containing 200 mL sterile ultrapure water supplemented with 5 % mineral salt medium (MSM; 4.3 g/L K_2HPO_4; 1.7 g/L KH_2PO_4; 2.69 g/L NH_4Cl; 0.2 g/L $MgCl_2$; 0.2 g/L yeast extract) (Afzal et al., 2007; Cai et al., 2021). Five incubation experiments were conducted: soil control; soil + Cu; soil + Cys; soil + Cys + Cu; and sterile soil + Cys + Cu (soil sterilized by autoclaving at 121 °C for 20 min). The soils were incubated aerobically at 30 °C for 14 days in a biochemical incubator (SPX-150, SH-ZUOLE, China) without shaking. The initial concentrations of cysteine and Cu (II) were 500 μM and 200 μM, respectively. All incubation experiments were carried out in triplicate.

2.2. Sampling and analysis of soil solution and solid phase

The incubation vials from different series were sacrificed at days 0, 1, 3, 5, 7, and 14. The soil suspensions were passed through 0.45-μm nylon filters (Anpel, China). The solution pH and Eh were measured using a pH meter (S220, Mettler Toledo, Switzerland) and an ORP meter (SX751, San-xin, China), respectively. Aliquots of the filtered solution were used to determine the dissolved organic carbon (DOC) content by a total organic carbon/total nitrogen analyzer (Multi 3100, Analytikjena, Germany). The sulfate concentration in the soil solution was measured using ion chromatography (MIC, Metrohm, Switzerland). Further aliquots were acidified (5 % HNO_3) for the measurement of Cu, Fe, and Mn ions using inductively coupled plasma optical emission spectrometry (ICP-OES; 5110, Agilent, USA). The sulfide concentration in the soil solution was determined according to previous studies (Cline, 1969; Thomas and Gaillard, 2017). Briefly, 500 μL of the filtered solution was added into a 2.0 mL centrifuge tube pre-filled with 100 μL of 5 M NaOH. Then, 200 μL of 2.6 % zinc acetate was added and the centrifuge tube was shaken thoroughly. Subsequently, 200 μL of 20 mM N, *N*-dimethyl-p-phenylenediamine sulfate in 7.2 N HCl and 200 μL of 20 mM $FeCl_3$ in 1.2 N HCl were added successively to the centrifuge tube. The OD_{670} was measured after 30 min.

The morphology and composition of the metal nanoparticles in the soil solid after incubation were determined using an emission transmission electron microscope-energy dispersive spectrometer (TEM-EDS). The soil was sampled and freeze-dried after reaction. A small amount of dried soil was selected with a toothpick and placed into a 2 mL centrifuge tube, to which 1.5 mL of ethanol was added. After homogenization by ultrasound for at least 30 s, 5 μL of soil suspension was pipetted onto a gold TEM grid. Finally, the gold grid was dried and transferred into the TEM chamber. TEM imaging and EDS analysis were performed in a Talos F200X G2 TEM operated at 200 kV. High-resolution TEM (HRTEM) and corresponding fast Fourier transform (FFT) analysis were used to characterize the crystal structure of the formed nanoparticles.

2.3. Isolation and characterization of cysteine-mineralizing strains from the paddy soil

The paddy soil sample was suspended in sterilized ultrapure water and diluted 100 times. Then, 50 μL of the diluted suspension was plated onto a beef extract peptone medium consisting of 5.0 g/L beef extract, 5.0 g/L peptone, 3.0 g/L yeast extract, 2.0 g/L NaCl, and 15 g/L agar. The petri dish was cultured upside-down at 30 °C for 2 d. We picked different single colonies for isolation based on their shape and size. The isolated microorganisms were plated onto a beef extract peptone medium supplemented with 1.0 g/L cysteine and 0.1 g/L Cu(II), and were cultured upside-down at 30 °C for 3–5 d. The cysteine-mineralizing microorganisms were screened by observing black colonies in agar medium.

One of the strains that formed a strong black colony was identified by sequencing the 16S rRNA gene. It was characterized for involvement in the copper sulfide production process via the cysteine-mineralization pathway. The strain was cultured in 100 mL of beef extract peptone medium at 30 °C for 24 h and then the precipitates were collected by centrifugation (4000 g, 20 min). The precipitates were washed twice and resuspended in 0.9 % NaCl. The cell suspension was transferred into a sterile mineral salt medium supplemented with 0.2 g/L yeast extract to achieve half of the initial OD_{600}. Three series of suspensions were made, with additions of 1) 2 mM of cysteine, 2) 200 μM of Cu(II), and 3) 2 mM of cysteine + 200 μM of Cu(II). Samples from these series were taken

after 0, 5, 10, 24, 36, 48, and 72 h of exposure to determine the sulfide and Cu concentrations in the solutions.

Thin-section sample of metal nanoparticles associated with microbial cells was analyzed using TEM-EDS. The microbial cells were collected by centrifugation and washed three times by phosphate buffer solution. The cells were then dehydrated for 15 min in ethanol solutions of increasing concentration (30 %, 50 %, 70 %, 90 %, 100 %). The cells were encapsulated by resin and set in an oven at 60 °C for 24 h. Finally, the encapsulated microbial cells were cut with a diamond knife microtome (Leica EM UC7FC7 Ultracut). The section was collected onto a gold TEM grid for TEM-EDS analysis.

2.4. Shotgun metagenomic sequencing and analysis of functional genes and microorganisms in the soil

We selected three samples for shotgun metagenomic DNA sequencing and analysis: 1) soil at day 0, 2) soil + Cys at day 7, and 3) soil + Cys + Cu at day 7. These samples are referred to as soil_0, soil_Cys_7, and soil_Cys_Cu_7, respectively. Total genomic DNA was extracted using the E.Z.N.A.® Soil DNA Kit (Omega Bio-tek, Norcross, GA, USA) according to the manufacturer's instructions. The concentration and purity of extracted DNA were determined by TBS-380 and NanoDrop2000 apparatus, respectively. DNA extract quality was checked on 1 % agarose gel. Metagenomic libraries were sequenced on an Illumina MiSeq at Majorbio in Shanghai, China and yielded 111–153 million reads per sample. The raw reads of the metagenome samples were quality-trimmed using fastq v0.20.0 software to remove low-quality reads. Specifically, fastq was used to cut the adapter sequence at the 3′ and 5′ ends of the sequence, and to remove reads with lengths < 50 bp, average mass value < 20, or containing N bases. The high quality of the paired-end and single-end reads was retained. The short-fragment sequences were assembled individually using megahit software (Li et al., 2015). Open reading frames (ORFs) were predicted using Prodigal software (Hyatt et al., 2010). CD-HIT software was used to cluster the predicted gene sequences to construct a non-redundant gene set (Fu et al., 2012). The gene abundance was calculated using SOAPaligner software (Li et al., 2009). Gene abundances were defined as the number of reads per million sequences to eliminate the influences of differences in sequencing data volume and gene length. Genes were annotated with biological functions using Diamond v0.8.35 software (parameters: blastp; E-value ≤ 1e-05) by comparing against the KEGG database (Buchfink et al., 2015). The data were analyzed on the online Majorbio Cloud Platform (https://www.majorbio.com).

2.5. Data availability

The metagenomic sequence data have been submitted to the National Center for Biotechnology Information Sequence Read Archive (NCBI SRA) and are available under BioProject accession number PRJNA889980.

3. Results

3.1. Dynamics of sulfide production and consumption in a cysteine-spiked paddy soil

Firstly, the ability of a local paddy soil to produce sulfide from cysteine (Cys) was determined to study the significance of organic sulfur mineralization in the environment. Fig. 1a shows the dynamics of the dissolved sulfide concentration during the 14 d of incubation. Soil samples incubated in the absence of cysteine produced little sulfide during this period. In the soil + Cys assay, sulfide was produced after 24 h and reached a peak of 169.3 μM on day 3. Sulfide concentrations were largely lower in the soil + Cys + Cu assay, peaking at 13.3 μM after 5 days. This result indicates that dissolved sulfide was captured and precipitated by copper ions. Consequently, the amount of sulfide

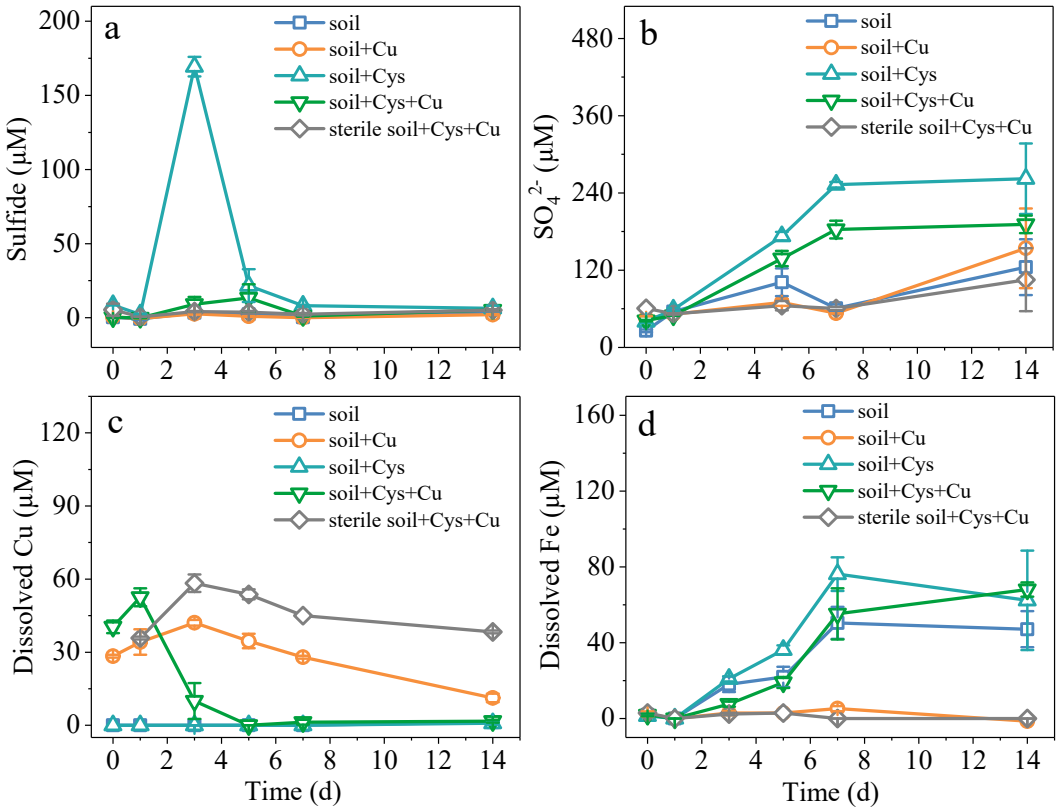

Fig. 1. Temporal changes in dissolved sulfide (a), SO_4^{2-} (b), Cu (c), and Fe (d) during incubation in soil, soil + Cu, soil + Cys, soil + Cys + Cu, and sterile soil + Cys + Cu assays. Points and error bars represent the means and standard deviations, respectively, of experimental triplicates.

released decreased sharply after 7 days, with consumption rates of 11.5 μM/d/g soil and 3.0 μM/d/g soil for the soil + Cys and soil + Cys + Cu assays, respectively. Meanwhile, in the control batch of sterile soil supplemented with cysteine and Cu(II), only very low amounts of sulfide were produced. This reveals the important role of microorganisms in this organic sulfur mineralization process. The concentration of SO_4^{2-} increased over time to 252.8 and 183.2 μM in the soil + Cys and soil + Cys + Cu assays, respectively (Fig. 1b). These increased SO_4^{2-} concentrations accompanied decreased sulfide concentrations, indicating that the dissolved sulfide was oxidized to sulfate, potentially via intermediate sulfur species.

3.2. Dynamics of dissolved Cu, Fe and Mn during soil incubation

Fig. 1c shows the dissolved Cu concentrations in soil solutions during the 14 days of incubation. The concentrations of total dissolved Cu in the soil and the soil + Cys assays were below 1.25 μM. In the soil + Cys + Cu assay, the Cu concentration decreased sharply from 52.5 μM to 10.0 μM during the first three days. At the fifth day of exposure, Cu was no longer detected. This could be attributed to the capture and precipitation of Cu ions by dissolved sulfide, which was produced during the first five days. The decrease in the dissolved Cu concentration also explains the significantly lower concentration of dissolved sulfide detected in the soil + Cys + Cu assay than in the soil + Cys assay (Fig. 1a). The Cu concentrations slowly decreased during soil incubation and remained at 11.3 μM in the soil + Cu assay and 38.3 μM in the sterile soil + Cys + Cu assay after 14 days.

In addition, steady increases in the concentrations of dissolved Fe and Mn were observed during the first 7 days of incubation. This is ascribed to microbially induced reductive dissolution of Fe and Mn oxides (Fig. 1d and Fig. S1). The obviously higher concentrations of dissolved Fe and Mn in cysteine-spiked soil after the hydrogen sulfide production phase indicate that hydrogen sulfide reduced Fe and Mn oxides abiotically. A significantly lower concentration of dissolved Fe in the soil + Cu assay might result from Cu toxicity. The earlier increase in the dissolved Mn concentration, as compared to the Fe concentration, is consistent with the finding that microbial respiration of Mn oxides (as terminal electron acceptors) occurs prior to the reduction of Fe oxides.

3.3. Formation of copper sulfide nanoparticles in the soil solid phase

The TEM results show that dispersed and spherical metal nanoparticles were formed in the soil + Cys + Cu assay during incubation (Fig. 2a). The diameters of the nanoparticles were 11.3–78.8 nm with an average of 37.6 nm based on measurements of 45 randomly selected particles. EDS point analysis indicates that the nanoparticles were

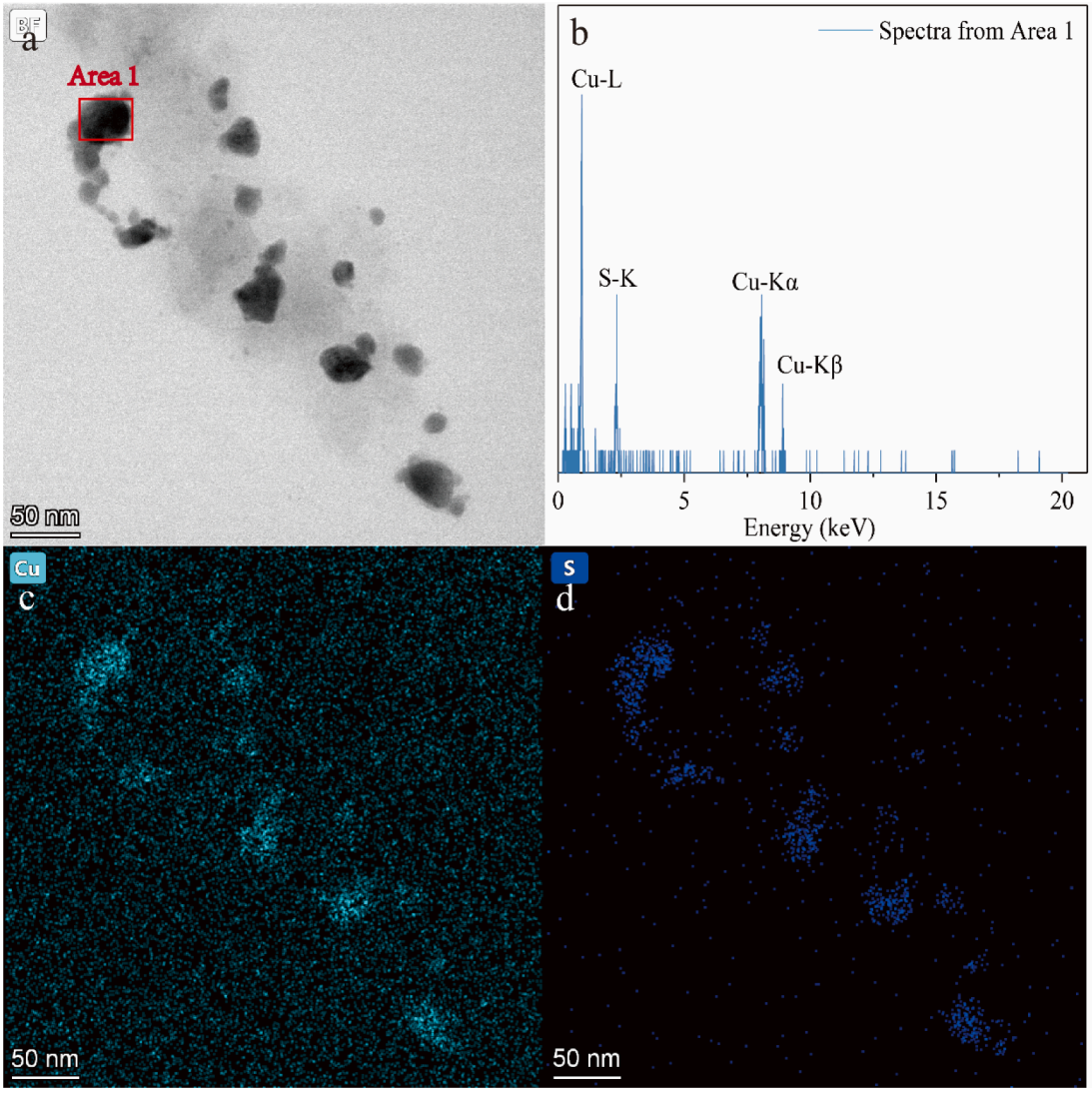

Fig. 2. (a) TEM micrographs of metal nanoparticles after 7 days of incubation in the soil + Cys + Cu assay. (b) Energy dispersive X-ray spectra (EDS) obtained from Area 1 in (a). (c-d) EDS mappings of Cu and S.

composed of copper and sulfur, with a molar Cu:S ratio of 2:1 (Fig. 2b). The EDS mapping images also confirm that the electron-dense nanoparticles were rich in Cu and S elements and contained little Fe, O, and Si elements (Fig. 2c and 2d, Fig. S2), suggesting that copper sulfide nanoparticles were indeed formed *in situ* during soil incubation. The HRTEM result shows a visible lattice fringe in the copper sulfide particles produced in the soil + Cys + Cu assay (Fig. S3a), suggesting the formation of a crystalline phase. An interplanar crystal spacing of 0.1870 nm corresponds to the (12 0 4) plane of djurleite ($Cu_{1.94}S$). The corresponding FFT analysis of the nanoparticles also confirms this djurleite structure (Fig. S3b; Cheung et al., 2016).

3.4. Cell-associated copper sulfide production by isolated Bacillus sp. TR1

We obtained 48 bacterial isolates from a 100-fold dilution of the paddy soil. The cysteine-mineralizing bacteria were screened by observing black copper sulfide precipitation in an agar medium, which was produced by a reaction between copper ions and sulfide released from cysteine. The soil bacteria could be divided into four categories according to the patterns of colony formation on the plates: (1) The inside of the colony was all blackened with a slight black halo, indicating the diffusion of hydrogen sulfide gas (Fig. 3a). There were 13 strains of bacteria in this category. (2) A black outer ring was formed taking the incubation site as the centre, which included 22 strains (Fig. 3b). (3) Grey precipitation appeared in the colony and produced creeping hyphae, including 10 strains (Fig. 3c). (4) No black precipitation in the colony; this category only included three strains (Fig. 3d). Ninety-three percent of the isolates from the paddy soil were able to produce sulfide from cysteine. These results highlight that diverse bacteria of the indigenous paddy soil microbial population possess the ability of reduced organic sulfur mineralization.

An isolate possessing a strong cysteine-mineralization ability was characterized as *Bacillus* based on the 16S rRNA gene. The maximum likelihood phylogenetic tree derived from 16S rRNA gene sequences revealed similarity and homology of the isolate to known *Bacillus* species (Fig. S4). The isolate belongs to the phylum *Firmicutes* and was termed *Bacillus* sp. TR1. When *Bacillus* sp. TR1 grew in MSM medium supplemented with cysteine, sulfide was produced during 0–10 h, which was in the logarithmic growth period of the culture, and peaked at 23.6 μM (Fig. S5a and S5b). After 10 h, microbial growth entered a stable period and the sulfide concentration decreased gradually. These results demonstrate that cysteine degradation by *Bacillus* sp. TR1 produces sulfide. In the *Bacillus* sp. TR-1 + Cys + Cu assay, the dissolved Cu concentration decreased sharply from 195 μM to 11.0 μM during 24 h of microbial cell growth (Fig. S5c). The decrease in the dissolved Cu concentration could be the result of rapid precipitation via sulfide capture, forming copper sulfide. The TEM results prove the formation of cell-associated copper sulfide nanoparticles after 48 h of incubation (Fig. 4a). The EDS results show that the cell-associated nanoparticles were mainly composed of Cu and S (Fig. 4b-d). The XRD pattern of the *Bacillus* sp. TR1 + Cys + Cu sample shows the major peaks at 33.875°, 36.296°, 37.425°, 40.719°, and 41.423° that can be attributed to the

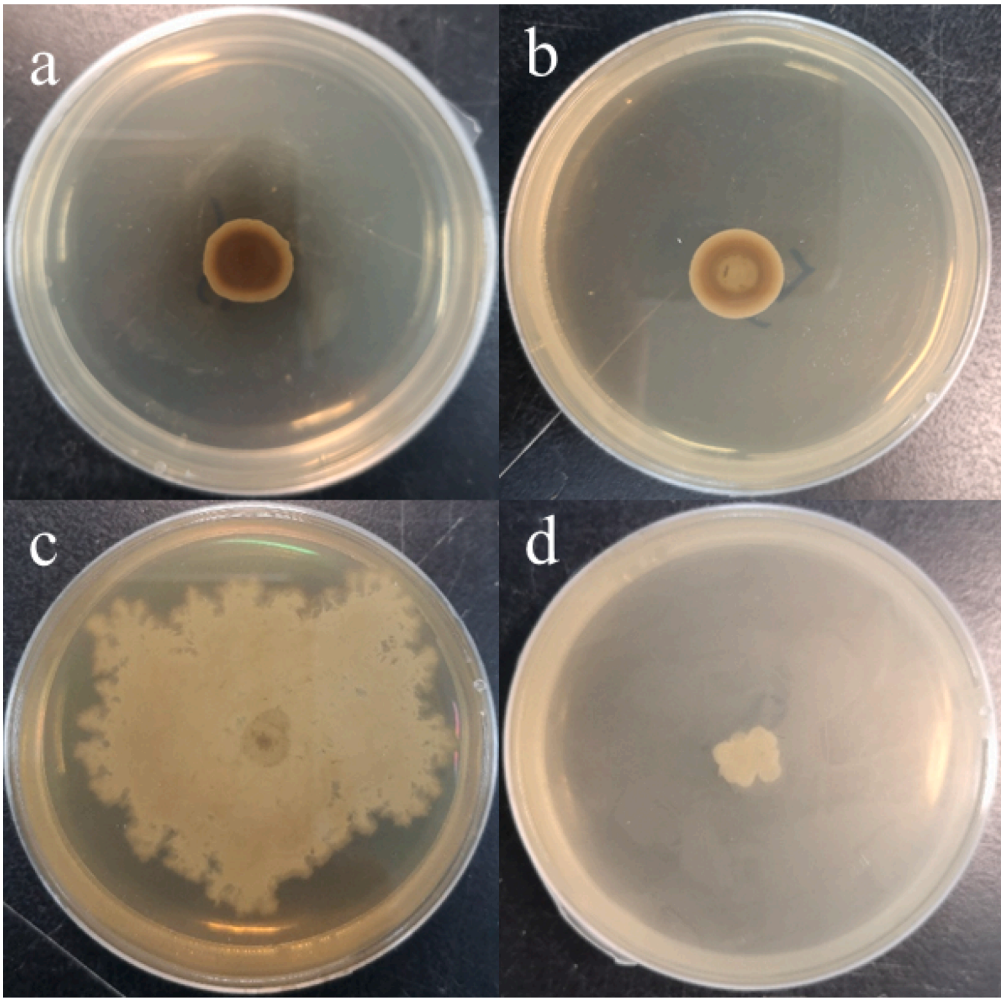

Fig. 3. Colonies of bacteria isolated from paddy soil grown on agar plates supplemented with cysteine and Cu. Colonies appeared black due to the copper sulfide precipitation, reflecting the differential cysteine-mineralization abilities of soil bacteria.

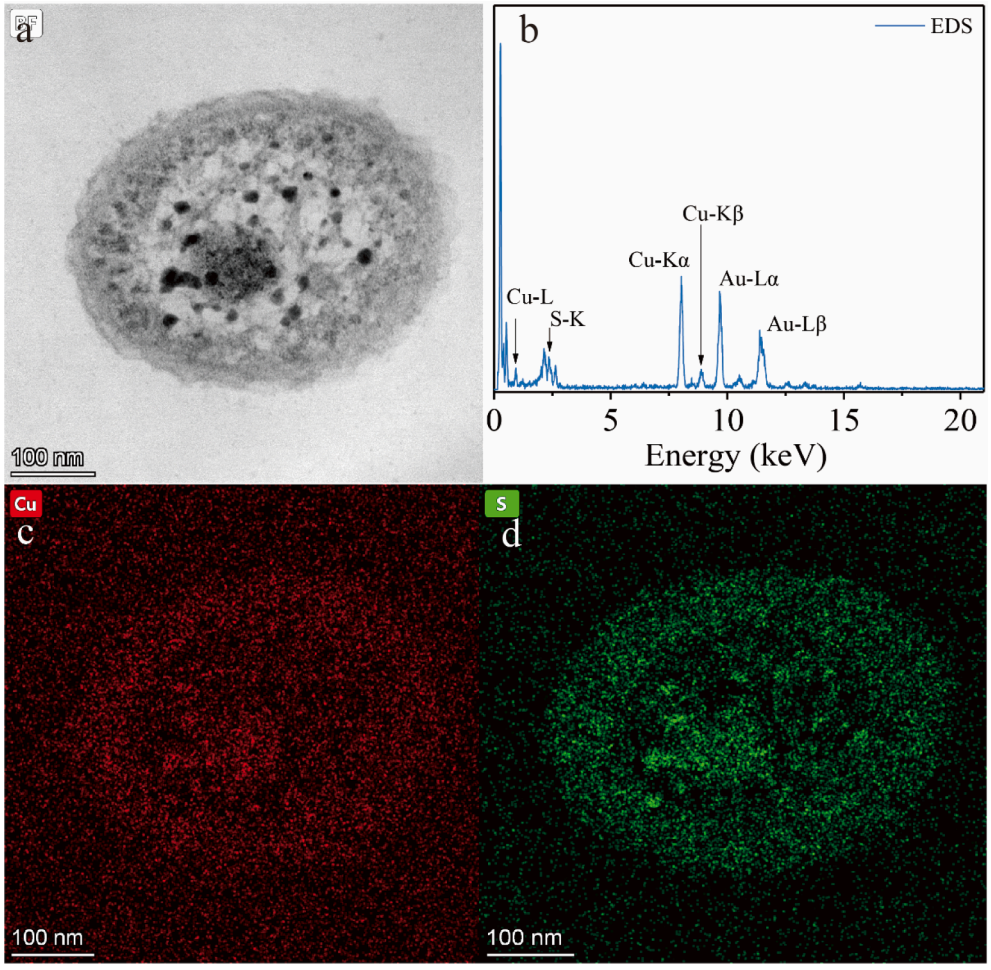

Fig. 4. (a) Cell-associated copper sulfide nanoparticles formed after 48 h of incubation of the *Bacillus* sp. TR1 isolated from paddy soil in MSM medium supplemented with cysteine and Cu. (b) Energy dispersive X-ray spectra (EDS) obtained from the cell-associated nanoparticles. (c-d) EDS mappings of Cu and S.

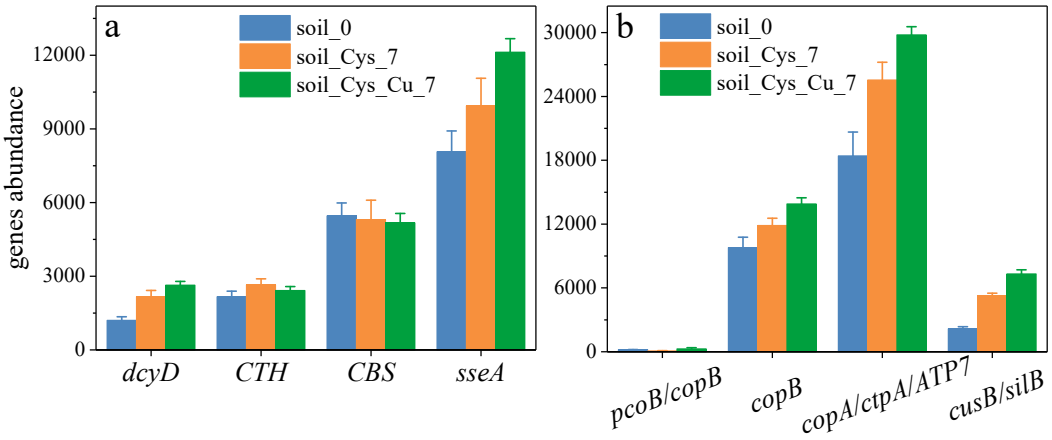

Fig. 5. Gene abundance changes for cysteine mineralization (a) and copper resistance (b). *dcyD*: cysteine desulfhydrase; *CTH*: cystathionine γ-lyase; *CBS*: cystathionine β-synthase; *sseA*: 3-mercaptopyruvate sulfurtransferase; *pcoB/copB*: copper resistance protein B; *copB*: P-type Cu^{2+} transporter; *copA/ctpA/ATP7*: P-type Cu^{+} transporter; *cusB/silB*: copper/silver efflux system. soil_0: paddy soil sample at 0 day; soil_Cys_7: enrichment with cysteine at 7 days; soil_Cys_Cu_7: enrichment with cysteine and Cu at 7 days.

(303), (400), (223), (321), and (224) crystallographic planes, respectively, of $Cu_{1.92}S$ (JCPDS 30-0505; Fig. S6b). These results provide direct evidence of cysteine degradation and copper sulfide formation via microbial metabolic processes.

3.5. Metagenomics analysis of genes for sulfur transformation and copper resistance

Pure culture techniques cannot fully demonstrate the characteristics of cysteine-mineralizing microbiota because most soil microorganisms

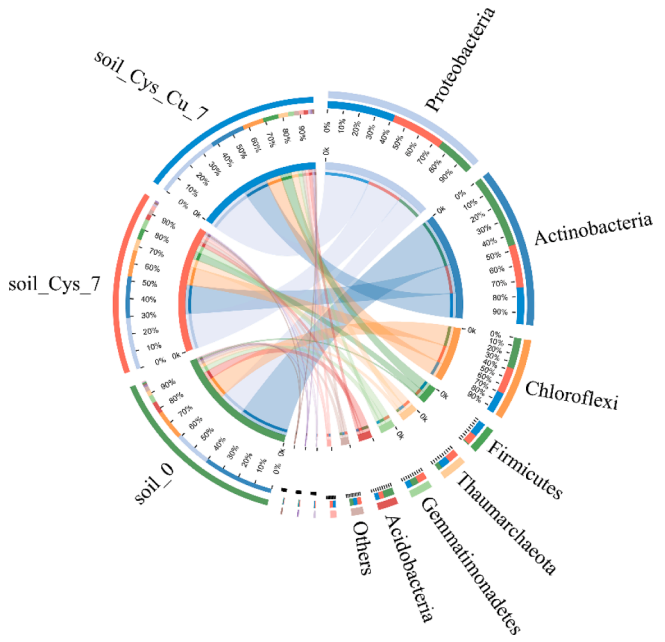

Fig. 6. Diversity and abundance of cysteine-mineralizing microorganisms at phylum level in the soil_0, soil_Cys_7, and soil_Cys_Cu_7 assays. Left half represents the abundance of species in the corresponding assay. Different colors on the left represent different species, while widths and values represent the species abundance in the corresponding assay. Right half shows the distribution proportion of phylum level in the three assays. Green, red, and blue arcs represent the proportions in assays soil_0, soil_Cys_7, and soil_Cys_Cu_7, respectively. Widths and values represent the proportions of corresponding phyla in the assays. (For interpretation of the references to colour in this figure legend, the reader is referred to the web version of this article.)

are not culturable. Therefore, metagenomics was applied to analyze the functional genes and associated microorganisms responsible for copper sulfide formation through cysteine mineralization. Genes related to cysteine mineralization and copper resistance were selected for detailed analysis. The enzymes responsible for cysteine mineralization, including cysteine desulfhydrase (EC: 4.4.1.15), cystathionine γ-lyase (EC: 4.4.1.1), cystathionine β-synthase (EC: 4.2.1.22), and 3-mercaptopyruvate sulfurtransferase (EC: 2.8.1.2), are encoded by *dcyD*, *CTH*, *CBS*, and *sseA* genes, respectively. The gene abundances were defined as the number of reads per million sequences, which is one of the most common methods for comparing the functional gene abundances of different samples. Many previous studies have measured read numbers to analyze carbon metabolism, nitrogen metabolism, and antimicrobial resistance in the environment (Gao et al., 2021; Gweon et al., 2019; Nadeau et al., 2019). Fig. 5a shows that the four cysteine mineralization genes were abundant in the paddy soil at day 0. This indicates that the indigenous microbial community of this environment has the ability to produce sulfide from cysteine. The *sseA* gene abundance was much higher than those of *dcyD*, *CTH*, and *CBS* in the soil_0 assay. After 7 days of incubation, the *sseA* gene abundance largely increased in the soil + Cys and soil + Cys + Cu assays. The *dcyD* gene abundance was approximately double-enriched at 7 days compared to day 0 in both the soil + Cys and soil + Cys + Cu assays. However, the *CTH* gene abundance displayed a slight increase while the *CBS* gene abundance decreased during soil incubation. These results indicate that in the investigated soil, 3-mercaptopyruvate sulfurtransferase and cysteine desulfhydrase played more important roles in producing sulfide from cysteine than cystathionine γ-lyase and cystathionine β-synthase.

Some of the copper resistance genes were detected in the paddy soil at day 0, including *pcoB/copB* (copper resistance protein B), *copB* (P-type Cu^{2+} transporter), *copA/ctpA/ATP7* (P-type Cu^{+} transporter), and *cusB/silB* (membrane fusion protein, copper/silver efflux system). Fig. 5b shows the changes in abundance of copper resistance genes in the assays of soil_0, soil_Cys_7, and soil_Cys_Cu_7. The P-type Cu^{+} transporter (60.3 %) showed a higher percentage of abundance in the soil at day 0 than the P-type Cu^{2+} transporter (32.0 %), the copper/silver efflux system (7.1 %), and the copper resistance protein B (0.6 %). All of the copper resistance gene abundances were increased by factors of 1.4–3.4 after 7 days of incubation in the soil + Cys + Cu assay, indicating that the soil microbial community could duplicate and express such copper resistance genes to avoid copper toxicity and maintain its survival and activity.

3.6. Taxonomic diversity of cysteine-mineralizing microorganisms

Taxonomic analysis of the cysteine mineralization metagenome indicates that the microbial community was dominated by bacteria (92.3 %), with a few archaea (7.7 %). The microbes with metabolic potential for cysteine mineralization in the paddy soil were highly diverse and included *Actinobacteria* (40.9 %), *Proteobacteria* (21.1 %), *Chloroflexi* (17.5 %), *Acidobacteria* (6.9 %), *Gemmatimonadetes* (4.5 %), *Thaumarchaeota* (2.9 %), and *Firmicutes* (0.7 %; Fig. 6). After 7 days of incubation, the abundances of the *Proteobacteria*, *Firmicutes*, and *Thaumarchaeota* phyla were greater in the soil with added cysteine, which stimulated the microbial community (Fig. 6).

Fig. 7 shows the top 15 genera with metabolic potential for cysteine mineralization via 3-mercaptopyruvate sulfurtransferase and cysteine desulfhydrase, based on species and function contribution analysis. The *sseA* gene for 3-mercaptopyruvate sulfurtransferase was identified in *Nitrososphaera*, *Phycicoccus*, *Candidatus* Nitrosocosmicus, *Noviherbaspirillum*, *Micromonospora*, *Sulfuriferula*, *Pseudolabrys*, *Gaiella*, *Geobacter*, and *Streptomyces*. After 7 days of incubation, the dominant genera in the paddy soil were *Sulfuriferula* (6.9 %), *Nitrososphaera* (5.9 %),

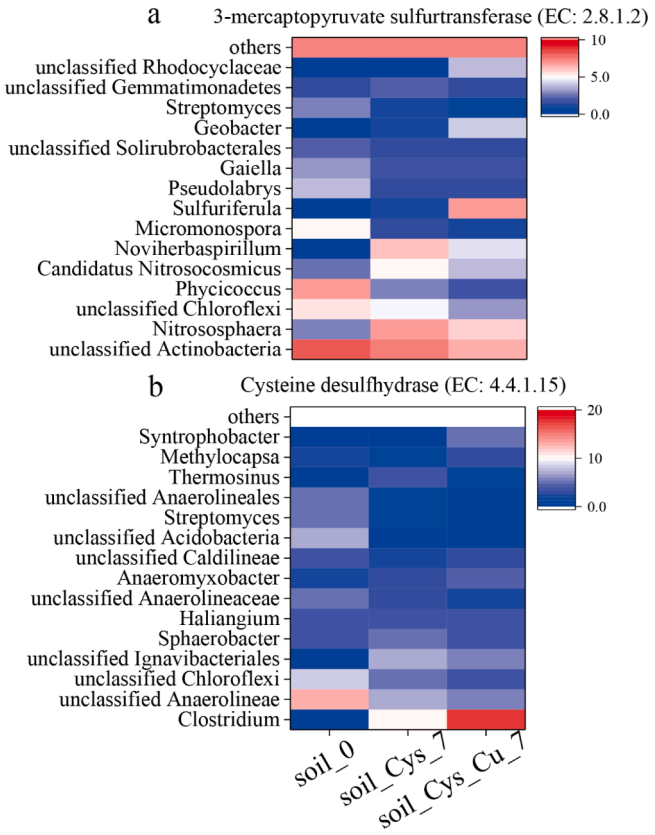

Fig. 7. Abundance of the top 15 genera with the metabolic potential for cysteine mineralization through 3-mercaptopyruvate sulfurtransferase (a) and cysteine desulfhydrase (b) in the soil_0, soil_Cys_7, and soil_Cys_Cu_7 assays.

Noviherbaspirillum (4.5 %), and *Geobacter* (4.3 %), indicating that these genera were the main producers of sulfide from cysteine via 3-mercaptopyruvate sulfurtransferase. The *dcyD* gene encoding cysteine desulfhydrase was found in *Clostridium*, *Sphaerobacter*, *Haliangium*, *Anaeromyxobacter*, *Streptomyces*, *Thermosinus*, *Methylocapsa*, and *Syntrophobacter*. *Clostridium* became the dominant genus after incubation in the soil_Cys_Cu_7 assay, indicating the importance of *Clostridium* for sulfide production via cysteine desulfhydrase. In addition, genes for cysteine mineralization were found in many unclassified microorganisms, suggesting that our knowledge of the phylogeny of cysteine-mineralizing microorganisms remains limited. It is also worth noting that the abundance of the *Bacillus* sp. TR1 isolated from pristine soil by MSM medium was lower than those of the above genera measured by the metagenome method. This might be attributable to the limitation of the pure culture technology for this microorganism. The microbial isolation and pure culture techniques could not enrich many of the unculturable strains in the soil. Hence, the strains that can be enriched in pure culture are highly dependent on the culture conditions, such as the medium composition and temperature. Even though *Bacillus* sp. TR1 was not the dominant cysteine-degrading bacterium, its physiological characteristics, ecosystem functions, and metabolic processes could still be representative.

4. Discussion

This study assessed the ecological functions of soil microbes participating in cysteine mineralization related to the sulfur cycle and copper transformation in a paddy soil. Our findings indicate that the inorganic sulfur resulting from organic sulfur mineralization reacts with Cu(II) to form copper sulfide, subsequently promoting copper immobilization. A combination of pure culturing of isolates and metagenomic analysis of related genes and microbes further revealed that this sulfur-copper reaction is driven by soil microbes, which are taxonomically diverse and have multiple ecological functions.

4.1. Cysteine mineralization drives a cryptic sulfur cycle

Our results show that the mineralization of carbon-bound S by microorganisms is an important source of inorganic sulfur, including sulfide and sulfate (Fig. 1a and 1b). Bacteria can cleave the R-SH bond using enzymes to release sulfide into pore water. Such reduced organic sulfur matter is thermodynamically easier to assimilate and the produced sulfide reacts with dissolved iron to form pyrite in the absence of sulfate reduction (Fakhraee and Katsev, 2019). Likewise, hydrolysis and mineralization of oxygen-bound S generates sulfate directly, providing a vital input of inorganic sulfur to low-sulfate environments that could support a substantial amount of sulfate reduction (Fakhraee et al., 2017).

The higher sulfate concentration in the soils supplemented with cysteine can be ascribed to oxidation of the sulfide that was produced by cysteine mineralization (Fig. 1a and 1b). Such sulfide oxidation would occur through both abiotic and biotic pathways. Sulfide is oxidized abiotically by oxygen, Fe oxides, and Mn oxides (Findlay et al., 2020), which resulted in the higher concentrations of dissolved Fe and Mn in the soil + Cys assay than in the soil assay (Fig. 1d and Fig. S1). Although Mn reacts with sulfide more rapidly than Fe, Fe might contribute more to sulfide oxidation due to its greater concentration in the soil (Holmkvist et al., 2011). Electron transfer between sulfide and ferric hydroxides leads to the formation of secondary iron (sulfide) minerals, and the Fe(III):$S(-II)_{aq}$ ratio controls the kinetics of pyrite formation during this diagenetic process (Wan et al., 2017). Sulfide can also react abiotically with organic matter to form organic sulfur, contributing to carbon preservation in sediments (Raven et al., 2021).

In the case of biotic oxidation processes, we detected the presence of sulfide-oxidizing enzymes such as sulfide:quinone oxidoreductase (SQR), sulfide dehydrogenase, and persulfide dioxygenase (PDO) (Reinartz et al., 1998; Xia et al., 2017) in the paddy soil using the metagenomic method (Fig. S7). The *sqr* gene encoding sulfide:quinone oxidoreductase was much more abundant than sulfide dehydrogenase and persulfide dioxygenase, and was largely enriched during soil incubation. This indicates that the sulfur-oxidizing microorganisms took part in the sulfide oxidization processes. Sulfide oxidization could be coupled with oxygen or nitrate reduction via long-distance electron transfer by cable bacteria of the family *Desulfobulbaceae* (Sandfeld et al., 2020).

The elevated sulfate concentrations resulting from sulfide oxidation can stimulate sulfate reduction due to increased promotion of sulfate availability (Sandfeld et al., 2020). This process accounts for the increased gene abundances associated with sulfate reduction pathways (Fig. S7). Sulfate reduction and sulfide oxidation are cyclic and, thus, invisible, constituting a cryptic sulfur cycle (Holmkvist et al., 2011). Sulfur intermediates such as sulfite and thiosulfate might also take part in this cryptic sulfur cycle because genes encoding sulfite/thiosulfate oxidation and reduction enzymes were detected and enriched during soil incubation (Fig. S7). This study demonstrates that organic sulfur molecules are important sources of inorganic sulfur input and that sulfur intermediates can act as biogeochemical hubs, thus driving a cryptic sulfur cycle.

4.2. Cysteine-mediated copper transformation and immobilization

The trends in dissolved Cu concentration show that Cu was captured and precipitated by dissolved sulfide produced through cysteine mineralization (Fig. 1c). That was accompanied by the production of dispersed and spherical Cu_xS nanoparticles during soil incubation (Fig. 2). Many previous studies also reported TEM observations of metal nanoparticle formation in soil (Hofacker et al., 2013a; Hofacker et al., 2013b; Weber et al., 2009; Xia et al., 2018). For example, metallic Cu(0) nanoparticles were initially formed in flooded paddy soils, which then transformed into Cu_xS nanoparticles with a hollow-sphere-like morphology and mean size of 20–70 nm depended on soil incubation temperature (Hofacker et al., 2013b). EDS analysis confirmed that the nanoparticles were rich in copper and sulfur and potentially contained other heavy metals, such as Hg (Hofacker et al., 2013a).

On the interaction between cysteine and metal, a previous study reported that cysteine has a ligand role in increasing the bioavailability of Cu to algal cells by reducing Cu(II) to Cu(I) to form a Cys-Cu complex (Walsh et al., 2015). A high concentration of cysteine can release Cd(II) initially adsorbed on δ-MnO_2 and form a small amount of Cd-cysteine (Sun et al., 2020). Cysteines can also act as electron shuttles to enhance the reduction of iron oxyhydroxide through a thiol/disulfide cycle (Eitel and Taillefert, 2017). Despite cysteine's ligand role and ability to reduce heavy metals, the degradation of cysteine to sulfide should be considered to influence heavy metal speciation in the environment. This cysteine degradation process has only been reported in microbial pure culture conditions, in which the addition of cysteine promoted the formation of HgS on a cell surface/extracellular matrix or in cell cytoplasm via three bacteria (Thomas et al., 2018). Another study reported that H_2S released from cysteine by SRB activity contributed to the transformation of FeS to pyrite, which promoted mineral diagenesis (Donald and Southam, 1999). Our findings further expand our knowledge of such coupled effects between cysteine degradation and metal behaviour in real soil environments.

Such biomineralization of Cu controls its dynamics and bioavailability in soils. Many studies have shown that copper sulfide formation is dependent on sulfate reduction. In flooded soils, Cu(II) is rapidly reduced to Cu(I) and Cu(0) and then transformed into copper sulfide precipitate following the onset of sulfate reduction (Fulda et al., 2013a). This phenomenon effectively decreases the dissolved copper concentration, which helps to decrease the copper toxicity that is mainly induced by the reactive oxygen species produced by ionic Cu (Clar et al., 2016). The Cu-sulfide produced during flooding is more persistent and stable than Cu(0) in the reoxidation phase (Fulda et al., 2013a). Other

chalcophile metals, such as Cd and Pb, inevitably affect the Cu-sulfide formation and dissolution processes. For example, Cu is more readily captured by sulfide than other chalcophile metals because of the relative thermodynamic stability of CuS in soils with limited sulfate concentrations (Fulda et al., 2013b). During drainage, the presence of CdS restrains the oxidative dissolution of CuS due to the voltaic effect, in which copper sulfide has the higher electrochemical potential and acts as a cathode (Huang et al., 2021a). Our study found a novel copper sulfide formation mechanism based on the reduced organic sulfur (cysteine) mineralization that is independent of sulfate reduction. This should be considered in analyses of copper dynamics in the environment. This organic sulfur mineralization pathway has application potential for the engineered microbial remediation of heavy metals. For example, organic sulfur-loaded materials or fertilizers could be amended into soil to stimulate indigenous microbial activity that immobilizes and stabilizes heavy metals.

4.3. *Cysteine-mineralizing microbes are diverse and have metabolic versatility*

The metagenomics results show the taxonomical diversity of the cysteine-mineralizing microorganisms that harbour genes encoding enzymes that liberate sulfide from cysteine (Fig. 6). *Actinobacteria*, *Proteobacteria*, and *Chloroflexi* were the most abundant phyla in the paddy soil, but only *Proteobacteria* was enriched during soil incubation when cysteine was supplied. This indicates that *Proteobacteria* plays a dominant role in cysteine mineralization and copper sulfide formation. *Firmicutes* and *Thaumarchaeota* also participate in these processes because of their increased abundance.

The enzymes 3-mercaptopyruvate sulfurtransferase and cysteine desulfhydrase contributed more to cysteine mineralization in the paddy soil than other enzymes because of the increased gene abundance (Fig. 5a). The genera *Geobacter* (Phylum *Proteobacteria*), *Sulfuriferula* (Phylum *Proteobacteria*), *Nitrososphaera* (Phylum *Thaumarchaeota*), and *Noviherbaspirillum* (Phylum *Proteobacteria*) were the main contributors to the encoding of 3-mercaptopyruvate sulfurtransferase, while *Clostridium* (Phylum *Firmicutes*) was the most important genus encoding cysteine desulfhydrase during soil incubation. These genera also played crucial roles in resisting copper toxicity because of their increased contributions to encoding copper-resistance systems in the paddy soil (Fig. S8). This indicates that they make dominant contributions to both sulfide production and heavy metal resistance, thus promoting the formation of copper sulfide nanoparticles in the soil.

The microorganisms enriched during soil incubation are important ecological contributors that link the sulfur, nitrogen, and metal cycles. Fig. 8 shows the putative metabolic pathways of cysteine mineralization that stimulate sulfur, nitrogen, and copper transformation in the paddy soil. The genera *Geobacter*, *Sulfuriferula*, *Nitrososphaera*, and *Noviherbaspirillum* degraded cysteine to pyruvate and sulfide in two steps through 3-mercaptopyruvate sulfurtransferase (*sseA*). In this pathway, cysteine was first converted to 3-mercaptopyruvate (3MP), then 3-mercaptopyruvate sulfurtransferase converted 3MP to pyruvate and sulfide (Shatalin et al., 2011). Cysteine was also transformed to sulfide through cysteine desulfhydrase (*dcyD*) by *Clostridium* with the formation of pyruvate and ammonia by-products (Morra and Dick, 1991). *Geobacter* and *Clostridium* has been reported as electroactive microorganisms that possess an extracellular electron transport (EET) capacity, which can mediate metal transformation and completely oxidize organic carbon (Lovley and Holmes, 2022). For example, *Geobacter* can reduce Cu(II) to Cu(I) and Cu(0) through the porin–cytochrome system and conductive nanowires (Qiu et al., 2020; Shi et al., 2016). The reaction between these copper species and sulfide from cysteine provides a Cu_xS formation pathway.

The metabolic activity of sulfide oxidation was confirmed by the increased gene abundance. The first sulfide oxidation pathway is the sulfide:quinone oxidoreductase pathway (*sqr*), which converts sulfide to elemental sulfur and thiosulfate (Xia et al., 2017). The Sox pathway is a multienzyme system that catalyses the oxidation of thiosulfate stepwise to sulfate (Vigneron et al., 2021). In addition, sulfide can also be oxidized to sulfate by the reverse sulfite reduction pathway (*dsrAB*). The enriched genus *Sulfuriferula* can grow autotrophically utilizing inorganic sulfur compounds (including sulfide, elemental sulfur, and thiosulfate) as electron donors, resulting in the oxidation of sulfide to sulfate (Watanabe et al., 2016). During this process, *Sulfuriferula* might couple sulfur oxidation with nitrate reduction in which reductase (*napAB*, *nirK*, *nirS*, *norB*, and *nosZ*) catalyses the reduction of nitrate to nitrite, N_2, or ammonium (Bell et al., 2020; Liang et al., 2020). The enriched genus *Noviherbaspirillum* has been reported to be capable of growing autotrophically by H_2-dependent denitrification and stepwise reduction of nitrate to N_2 (Xu et al., 2021). One of the by-products of cysteine mineralization is ammonia, which is a possible source of nitrate through oxidation (Martens-Habbena and Qin, 2022). *Nitrososphaera* is a typical

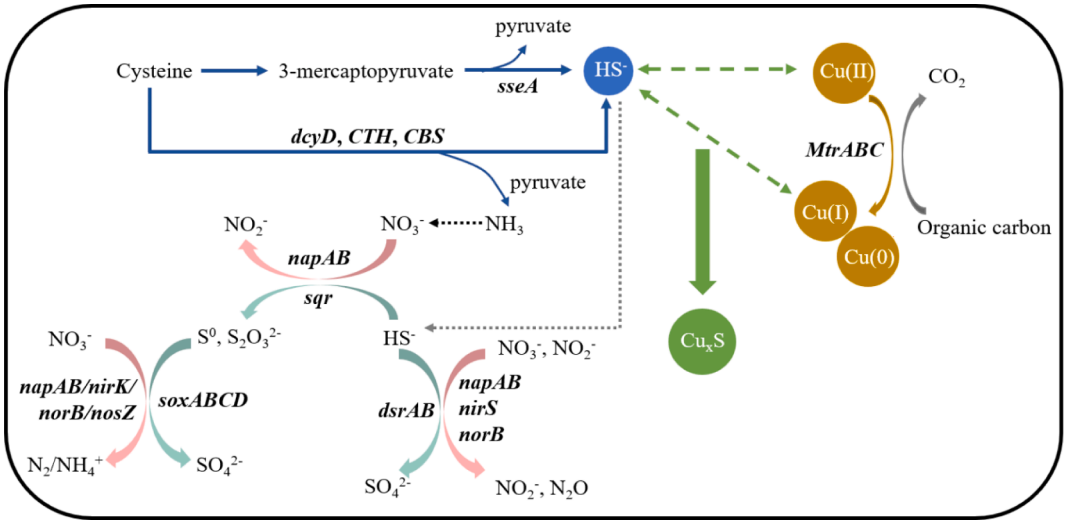

Fig. 8. Metabolic construction of the putative pathways for cysteine mineralization to drive sulfur cycling and copper sulfide formation. Coloured arrows indicate different metabolic pathways. Cysteine mineralization: blue; copper reduction: orange; copper sulfide formation: green; organic carbon oxidation: grey; anammox oxidation: black; S oxidation: cyan; N reduction: pink. (For interpretation of the references to colour in this figure legend, the reader is referred to the web version of this article.)

ammonia-oxidizing archaea (AOA) and performs the first and rate-limiting step of nitrification (Huang et al., 2021b). The enzymes for ammonia oxidation use copper as a cofactor to transport electrons and gain energy (Reyes et al., 2020). Therefore, these active microbes responsible for cysteine mineralization are metabolically versatile and take part in many biogeochemical reactions, including the carbon, sulfur, nitrogen, and metal cycles.

5. Conclusions

Unlike our extensive understanding of inorganic sulfur transformation, the way in which organic sulfur mineralization affects heavy metal behaviour in the environment remains largely unknown. The present study highlights the importance of cysteine mineralization in the formation of copper sulfide nanoparticles in paddy soils, which changes the mobility and bioavailability of copper. The transformation of cysteine to sulfide requires several microbial enzymes, with 3-mercaptopyruvate sulfurtransferase encoded by the *sseA* gene playing a dominant role in the investigated paddy soil. The produced sulfide was oxidized to sulfate through abiotic and biotic reactions to drive a cryptic sulfur cycle, or was captured by copper ions to cause copper sulfide precipitation. This is a new copper sulfide formation mechanism independent of sulfate reduction pathways. Our study further identified the diversity, abundance, and metabolic potential of the cysteine-mineralizing microbiota. The results show that a number of taxonomically diverse microorganisms carry genes encoding enzymes for cysteine mineralization, in which *Proteobacteria*, *Firmicutes*, and *Thaumarchaeota* were enriched during soil incubation. The most important genera for sulfide production were *Geobacter*, *Sulfuriferula*, *Nitrososphaera*, *Noviherbaspirillum*, and *Clostridium*, which are metabolically versatile and participate in metal resistance and reduction, sulfide oxidation, nitrification, and ammonia oxidation reactions. This enables them to survive and maintain active metabolism under unfavourable conditions. Overall, this study emphasizes the ecological functions of soil microbes in performing reduced organic sulfur mineralization, which controls the biogeochemical processes of copper.

Declaration of Competing Interest

The authors declare that they have no known competing financial interests or personal relationships that could have appeared to influence the work reported in this paper.

Data availability

Data will be made available on request.

Acknowledgments

This work was supported by the National Key Research & Development Program of China (No. 2018YFC1800600), the National Natural Science Foundation of China (No. 41877500, No. 41977115, and No. 42022057).

Appendix A. Supplementary data

Supplementary data to this article can be found online at https://doi.org/10.1016/j.geoderma.2022.116300.

References

Afzal, M., Iqbal, S., Rauf, S., Khalid, Z.M., 2007. Characteristics of phenol biodegradation in saline solutions by monocultures of *Pseudomonas aeruginosa* and *Pseudomonas pseudomallei*. J. Hazard. Mater. 149 (1), 60–66. https://doi.org/10.1016/j.jhazmat.2007.03.046.

Averill, B.A., 1996. Dissimilatory nitrite and nitric oxide reductases. Chem. Rev. 96 (7), 2951–2964. https://doi.org/10.1021/cr950056p.

Baath, E., 1989. Effects of heavy metals in soil on microbial processes and populations (a review). Water, Air, Soil Pollut. 47 (3), 335–379. https://doi.org/10.1007/BF00279331.

Bell, E., Lamminmaki, T., Alneberg, J., Andersson, A.F., Qian, C., Xiong, W., Hettich, R. L., Frutschi, M., Bernier-Latmani, R., 2020. Active sulfur cycling in the terrestrial deep subsurface. ISME J. 14 (5), 1260–1272. https://doi.org/10.1038/s41396-020-0602-x.

Buchfink, B., Xie, C., Huson, D.H., 2015. Fast and sensitive protein alignment using DIAMOND. Nat. Methods 12 (1), 59–60. https://doi.org/10.1038/nmeth.3176.

Cai, X., ThomasArrigo, L.K., Fang, X., Bouchet, S., Cui, Y., Kretzschmar, R., 2021. Impact of organic matter on microbially-mediated reduction and mobilization of arsenic and iron in arsenic(V)-bearing ferrihydrite. Environ. Sci. Technol. 55 (2), 1319–1328. https://doi.org/10.1021/acs.est.0c05329.

Cheung, T.L., Hong, L., Rao, N., Yang, C., Wang, L., Lai, W.J., Chong, P.H.J., Law, W.-C., Yong, K.T., 2016. The non-aqueous synthesis of shape controllable $Cu_{2-x}S$ plasmonic nanostructures in a continuous-flow millifluidic chip for the generation of photo-induced heating. Nanoscale 8 (12), 6609–6622. https://doi.org/10.1039/C5NR09144F.

Clar, J.G., Li, X., Impellitteri, C.A., Bennett-Stamper, C., Luxton, T.P., 2016. Copper nanoparticle induced cytotoxicity to nitrifying bacteria in wastewater treatment: A mechanistic copper speciation study by X-ray absorption spectroscopy. Environ. Sci. Technol. 50 (17), 9105–9113. https://doi.org/10.1021/acs.est.6b01910.

Cline, J.D., 1969. Spectrophotometric determination of hydrogen sulfide in natural waters. Limnol. Oceanogr. 14 (3), 454–458. https://doi.org/10.4319/lo.1969.14.3.0454.

Couture, R.-M., Fischer, R., Van Cappellen, P., Gobeil, C., 2016. Non-steady state diagenesis of organic and inorganic sulfur in lake sediments. Geochim. Cosmochim. Acta 194, 15–33. https://doi.org/10.1016/j.gca.2016.08.029.

Donald, R., Southam, G., 1999. Low temperature anaerobic bacterial diagenesis of ferrous monosulfide to pyrite. Geochim. Cosmochim. Acta 63 (13), 2019–2023. https://doi.org/10.1016/S0016-7037(99)00140-4.

Eitel, E.M., Taillefert, M., 2017. Mechanistic investigation of Fe(III) oxide reduction by low molecular weight organic sulfur species. Geochim. Cosmochim. Acta 215, 173–188. https://doi.org/10.1016/j.gca.2017.07.016.

Fakhraee, M., Katsev, S., 2019. Organic sulfur was integral to the Archean sulfur cycle. Nat. Commun. 10 (1), 4556. https://doi.org/10.1038/s41467-019-12396-y.

Fakhraee, M., Li, J., Katsev, S., 2017. Significant role of organic sulfur in supporting sedimentary sulfate reduction in low-sulfate environments. Geochim. Cosmochim. Acta 213, 502–516. https://doi.org/10.1016/j.gca.2017.07.021.

Findlay, A.J., Pellerin, A., Laufer, K., Jørgensen, B.B., 2020. Quantification of sulphide oxidation rates in marine sediment. Geochim. Cosmochim. Acta 280, 441–452. https://doi.org/10.1016/j.gca.2020.04.007.

Fu, L., Niu, B., Zhu, Z., Wu, S., Li, W., 2012. CD-HIT: accelerated for clustering the next-generation sequencing data. Bioinformatics 28 (23), 3150–3152. https://doi.org/10.1093/bioinformatics/bts565.

Fulda, B., Voegelin, A., Ehlert, K., Kretzschmar, R., 2013a. Redox transformation, solid phase speciation and solution dynamics of copper during soil reduction and reoxidation as affected by sulfate availability. Geochim. Cosmochim. Acta 123, 385–402. https://doi.org/10.1016/j.gca.2013.07.017.

Fulda, B., Voegelin, A., Kretzschmar, R., 2013b. Redox-controlled changes in cadmium solubility and solid-phase speciation in a paddy soil as affected by reducible sulfate and copper. Environ. Sci. Technol. 47 (22), 12775–12783. https://doi.org/10.1021/es401997d.

Gao, Y., Du, J., Bahar, M.M., Wang, H., Subashchandrabose, S., Duan, L., Yang, X., Megharaj, M., Zhao, Q., Zhang, W., Liu, Y., Wang, J., Naidu, R., 2021. Metagenomics analysis identifies nitrogen metabolic pathway in bioremediation of diesel contaminated soil. Chemosphere 271, 129566. https://doi.org/10.1016/j.chemosphere.2021.129566.

Gweon, H.S., Shaw, L.P., Swann, J., De Maio, N., AbuOun, M., Niehus, R., Hubbard, A.T. M., Bowes, M.J., Bailey, M.J., Peto, T.E.A., Hoosdally, S.J., Walker, A.S., Sebra, R.P., Crook, D.W., Anjum, M.F., Read, D.S., Stoesser, N., 2019. The impact of sequencing depth on the inferred taxonomic composition and AMR gene content of metagenomic samples. Environ. microbiome 14 (1), 7. https://doi.org/10.1186/s40793-019-0347-1.

Hofacker, A.F., Voegelin, A., Kaegi, R., Kretzschmar, R., 2013a. Mercury mobilization in a flooded soil by incorporation into metallic copper and metal sulfide nanoparticles. Environ. Sci. Technol. 47 (14), 7739–7746. https://doi.org/10.1021/es4010976.

Hofacker, A.F., Voegelin, A., Kaegi, R., Weber, F.-A., Kretzschmar, R., 2013b. Temperature-dependent formation of metallic copper and metal sulfide nanoparticles during flooding of a contaminated soil. Geochim. Cosmochim. Acta 103, 316–332. https://doi.org/10.1016/j.gca.2012.10.053.

Holmkvist, L., Ferdelman, T.G., Jørgensen, B.B., 2011. A cryptic sulfur cycle driven by iron in the methane zone of marine sediment (Aarhus Bay, Denmark). Geochim. Cosmochim. Acta 75 (12), 3581–3599. https://doi.org/10.1016/j.gca.2011.03.033.

Hou, D., O'Connor, D., Igalavithana, A.D., Alessi, D.S., Luo, J., Tsang, D.C.W., Sparks, D. L., Yamauchi, Y., Rinklebe, J., Ok, Y.S., 2020. Metal contamination and bioremediation of agricultural soils for food safety and sustainability. Nat. Rev. Earth Environ. 1 (7), 366–381. https://doi.org/10.1038/s43017-020-0061-y.

Huang, L., Chakrabarti, S., Cooper, J., Perez, A., John, S.M., Daroub, S.H., Martens-Habbena, W., 2021b. Ammonia-oxidizing archaea are integral to nitrogen cycling in a highly fertile agricultural soil. ISME Commun. 1 (1), 19. https://doi.org/10.1038/s43705-021-00020-4.

Huang, H., Chen, H.P., Kopittke, P.M., Kretzschmar, R., Zhao, F.J., Wang, P., 2021a. The voltaic effect as a novel mechanism controlling the remobilization of cadmium in paddy soils during drainage. Environ. Sci. Technol. 55 (3), 1750–1758. https://doi.org/10.1021/acs.est.0c06561.

Hyatt, D., Chen, G.-L., LoCascio, P.F., Land, M.L., Larimer, F.W., Hauser, L.J., 2010. Prodigal: prokaryotic gene recognition and translation initiation site identification. BMC Bioinf. 11 (1), 119. https://doi.org/10.1186/1471-2105-11-119.

Jorgensen, B.B., Findlay, A.J., Pellerin, A., 2019. The biogeochemical sulfur cycle of marine sediments. Front Microbiol 10, 849. https://doi.org/10.3389/fmicb.2019.00849.

Kertesz, M.A., Mirleau, P., 2004. The role of soil microbes in plant sulphur nutrition. J. Exp. Bot. 55 (404), 1939–1945. https://doi.org/10.1093/jxb/erh176.

Li, D., Liu, C.-M., Luo, R., Sadakane, K., Lam, T.-W., 2015. MEGAHIT: an ultra-fast single-node solution for large and complex metagenomics assembly via succinct de Bruijn graph. Bioinformatics 31 (10), 1674–1676. https://doi.org/10.1093/bioinformatics/btv033.

Li, R., Yu, C., Li, Y., Lam, T.-W., Yiu, S.-M., Kristiansen, K., Wang, J., 2009. SOAP2: an improved ultrafast tool for short read alignment. Bioinformatics 25 (15), 1966–1967. https://doi.org/10.1093/bioinformatics/btp336.

Liang, Y., Wei, D., Hu, J., Zhang, J., Liu, Z., Li, A., Li, R., 2020. Glyphosate and nutrients removal from simulated agricultural runoff in a pilot pyrrhotite constructed wetland. Water Res. 168, 115154 https://doi.org/10.1016/j.watres.2019.115154.

Lovley, D.R., Holmes, D.E., 2022. Electromicrobiology: the ecophysiology of phylogenetically diverse electroactive microorganisms. Nat. Rev. Microbiol. 20 (1), 5–19. https://doi.org/10.1038/s41579-021-00597-6.

Martens-Habbena, W., Qin, W., 2022. Archaeal nitrification without oxygen. Science 375 (6576), 27–28. https://doi.org/10.1126/science.abn0373.

Moran, M.A., Durham, B.P., 2019. Sulfur metabolites in the pelagic ocean. Nat. Rev. Microbiol. 17 (11), 665–678. https://doi.org/10.1038/s41579-019-0250-1.

Morra, M., Dick, W., 1989. Hydrogen sulfide production from cysteine (cystine) in soil. Soil Sci. Soc. Am. J. 53 (2), 440–444.

Morra, M.J., Dick, W.A., 1991. Mechanisms of H_2S production from cysteine and cystine by microorganisms isolated from soil by selective enrichment. Appl. Environ. Microbiol. 57 (5), 1413–1417. https://doi.org/10.1128/aem.57.5.1413-1417.1991.

Nadeau, S.A., Roco, C.A., Debenport, S.J., Anderson, T.R., Hofmeister, K.L., Walter, M.T., Shapleigh, J.P., 2019. Metagenomic analysis reveals distinct patterns of denitrification gene abundance across soil moisture, nitrate gradients. Environ. Microbiol. 21 (4), 1255–1266. https://doi.org/10.1111/1462-2920.14587.

Prietzel, J., Thieme, J., Salome, M., Knicker, H., 2007. Sulfur K-edge XANES spectroscopy reveals differences in sulfur speciation of bulk soils, humic acid, fulvic acid, and particle size separates. Soil Biol. Biochem. 39 (4), 877–890. https://doi.org/10.1016/j.soilbio.2006.10.007.

Prietzel, J., Botzaki, A., Tyufekchieva, N., Brettholle, M., Thieme, J., Klysubun, W., 2011. Sulfur speciation in soil by S K-Edge XANES spectroscopy: comparison of spectral deconvolution and linear combination fitting. Environ. Sci. Technol. 45 (7), 2878–2886. https://doi.org/10.1021/es102180a.

Qiu, H., Xu, H., Xu, Z., Xia, B., Peijnenburg, W., Cao, X., Du, H., Zhao, L., Qiu, R., He, E., 2020. The shuttling effects and associated mechanisms of different types of iron oxide nanoparticles for Cu(II) reduction by *Geobacter sulfurreducens*. J. Hazard. Mater. 393, 122390 https://doi.org/10.1016/j.jhazmat.2020.122390.

Raven, M.R., Keil, R.G., Webb, S.M., 2021. Microbial sulfate reduction and organic sulfur formation in sinking marine particles. Science 371 (6525), 178–181. https://doi.org/10.1126/science.abc6035.

Reinartz, M., Tschäpe, J., Brüser, T., Trüper, H.G., Dahl, C., 1998. Sulfide oxidation in the phototrophic sulfur bacterium *Chromatium vinosum*. Arch. Microbiol. 170 (1), 59–68. https://doi.org/10.1007/s002030050615.

Reyes, C., Hodgskiss, L.H., Kerou, M., Pribasnig, T., Abby, S.S., Bayer, B., Kraemer, S.M., Schleper, C., 2020. Genome wide transcriptomic analysis of the soil ammonia oxidizing archaeon *Nitrososphaera viennensis* upon exposure to copper limitation. ISME J. 14 (11), 2659–2674. https://doi.org/10.1038/s41396-020-0715-2.

Rubino, J.T., Franz, K.J., 2012. Coordination chemistry of copper proteins: how nature handles a toxic cargo for essential function. J. Inorg. Biochem. 107 (1), 129–143. https://doi.org/10.1016/j.jinorgbio.2011.11.024.

Sandfeld, T., Marzocchi, U., Petro, C., Schramm, A., Risgaard-Petersen, N., 2020. Electrogenic sulfide oxidation mediated by cable bacteria stimulates sulfate reduction in freshwater sediments. ISME J. 14 (5), 1233–1246. https://doi.org/10.1038/s41396-020-0607-5.

Semrau, J.D., DiSpirito, A.A., Yoon, S., 2010. Methanotrophs and copper. FEMS Microbiol. Rev. 34 (4), 496–531. https://doi.org/10.1111/j.1574-6976.2010.00212.x.

Shatalin, K., Shatalina, E., Mironov, A., Nudler, E., 2011. H_2S: a universal defense against antibiotics in bacteria. Science 334 (6058), 986–990. https://doi.org/10.1126/science.1209855.

Shi, L., Dong, H., Reguera, G., Beyenal, H., Lu, A., Liu, J., Yu, H.Q., Fredrickson, J.K., 2016. Extracellular electron transfer mechanisms between microorganisms and minerals. Nat. Rev. Microbiol. 14 (10), 651–662. https://doi.org/10.1038/nrmicro.2016.93.

Sun, Q., Cui, P., Wu, S., Liu, C., Fan, T., Alves, M.E., Cheng, H., Huang, M., Zhou, D., Wang, Y., 2020. Role of reduced sulfur in the transformation of Cd(II) immobilized by delta-MnO_2. Environ. Sci. Technol. 54 (23), 14955–14963. https://doi.org/10.1021/acs.est.0c02936.

Swaby, R.J., Fedel, R., 1973. Microbial production of sulphate and sulphide in some Australian soils. Soil Biol. Biochem. 5 (6), 773–781. https://doi.org/10.1016/0038-0717(73)90022-9.

Thomas, S.A., Gaillard, J.F., 2017. Cysteine addition promotes sulfide production and 4-fold Hg(II)-S coordination in actively metabolizing *Escherichia coli*. Environ. Sci. Technol. 51 (8), 4642–4651. https://doi.org/10.1021/acs.est.6b06400.

Thomas, S.A., Rodby, K.E., Roth, E.W., Wu, J., Gaillard, J.F., 2018. Spectroscopic and microscopic evidence of biomediated HgS species formation from Hg(II)-cysteine complexes: Implications for Hg(II) bioavailability. Environ. Sci. Technol. 52 (17), 10030–10039. https://doi.org/10.1021/acs.est.8b01305.

Vigneron, A., Cruaud, P., Culley, A.I., Couture, R.-M., Lovejoy, C., Vincent, W.F., 2021. Genomic evidence for sulfur intermediates as new biogeochemical hubs in a model aquatic microbial ecosystem. Microbiome 9 (1). https://doi.org/10.1186/s40168-021-00999-x.

Walsh, M.J., Goodnow, S.D., Vezeau, G.E., Richter, L.V., Ahner, B.A., 2015. Cysteine enhances bioavailability of copper to marine phytoplankton. Environ. Sci. Technol. 49 (20), 12145–12152. https://doi.org/10.1021/acs.est.5b02112.

Wan, M., Schröder, C., Peiffer, S., 2017. Fe(III):S(-II) concentration ratio controls the pathway and the kinetics of pyrite formation during sulfidation of ferric hydroxides. Geochim. Cosmochim. Acta 217, 334–348. https://doi.org/10.1016/j.gca.2017.08.036.

Watanabe, T., Kojima, H., Fukui, M., 2016. to *Sulfuriferula plumbiphila* corrig. Int. J. Syst. Evol. Microbiol. 66 (5), 2041–2045.

Weber, F.-A., Voegelin, A., Kaegi, R., Kretzschmar, R., 2009. Contaminant mobilization by metallic copper and metal sulphide colloids in flooded soil. Nat. Geosci. 2 (4), 267–271. https://doi.org/10.1038/ngeo476.

Wilhelm Scherer, H., 2009. Sulfur in soils. J. Plant Nutr. Soil Sci. 172 (3), 326–335. https://doi.org/10.1002/jpln.200900037.

Xia, Y., Lu, C., Hou, N., Xin, Y., Liu, J., Liu, H., Xun, L., 2017. Sulfide production and oxidation by heterotrophic bacteria under aerobic conditions. ISME J. 11 (12), 2754–2766. https://doi.org/10.1038/ismej.2017.125.

Xia, B., Qiu, H., Knorr, K.-H., Blodau, C., Qiu, R., 2018. Occurrence and fate of colloids and colloid-associated metals in a mining-impacted agricultural soil upon prolonged flooding. J. Hazard. Mater. 348, 56–66. https://doi.org/10.1016/j.jhazmat.2018.01.026.

Xu, Y., Teng, Y., Dong, X., Wang, X., Zhang, C., Ren, W., Zhao, L., Luo, Y., Greening, C., 2021. Genome-resolved metagenomics reveals how soil bacterial communities respond to elevated H_2 availability. Soil Biol. Biochem. 163, 108464 https://doi.org/10.1016/j.soilbio.2021.108464.

Zhang, J., Liu, R., Xi, S., Cai, R., Zhang, X., Sun, C., 2020. A novel bacterial thiosulfate oxidation pathway provides a new clue about the formation of zero-valent sulfur in deep sea. ISME J. 14 (9), 2261–2274. https://doi.org/10.1038/s41396-020-0684-5.